Chapter 4

Anisotropic expansion in a Gaussian density plasmasphere due to intense laser irradiation

The work included in this chapter is partly published in A. Bhagawati and N. Das, "Effect of density gradients on the generation of a highly energetic and strongly collimated proton beam from a laser-irradiated Gaussian shaped hydrogen microsphere", *Physics of Plasmas*, 29, 053107 (2022).

The interaction of an intense laser pulse with a relativistically transparent target leads to the expansion of the plasma target. This expansion mechanism is studied in this chapter in a density-modified spherical target. A Gaussian density variation is introduced in the radial direction having a peak value at the centre of the target sphere. The peak central density is kept around the relativistically critical value to ensure a fast expansion of the target. A micron-sized plasma sphere has shown an anisotropicity in the expansion. The anisotropic behaviour is favourable in the context of attaining energetic ions. The expansion mechanism has been identified to be ambipolar for the micron-sized target. Upon reduction in the target size the plasma expansion shifts from ambipolar to an isotropic Coulomb explosion.

4.1 Plasma expansion due to interaction with a laser pulse

In chapter 3, a Gaussian distribution of the plasma density in the micron-sized sphere showed promising results in terms of proton acceleration. It has thus become important to analyse the effects of the density modification in the dynamics of the protons after it gets hit by the laser pulse. Due to a gradually increasing density regime at the front laser-irradiated side of the sphere target, the laser absorption is enhanced [1, 2, 3, 4]. As the plasma electrons acquire energy from the intense laser pulse, their motion becomes relativistic and a new electron population termed 'hot electrons' are generated. A relativistically near-critically dense target helps in increasing the hot electron number as most of the electrons absorb the laser energy and gain momenta. The laser energy absorption by the electrons lead to the expansion of the plasma and in this chapter, the plasma expansion due to the laser action is studied when there is a radial density inhomogeneity in the target. The plasma ions are also affected by the electron motion and can get accelerated due to the expansion.

The plasma expansion depends on the temperature of the electrons after the interaction with the main laser pulse. For low electron temperatures, the quasi-neutrality of the plasma is maintained in the bulk of the plasma. In such cases, most of the electrons are held back by the charge separation field created by the massive ions at the plasma core. The Debye length $\lambda_D = \sqrt{\frac{T_e}{4\pi n_{e0} e^2}}$, is much smaller than the target size. Here, T_e and n_{e0} is the electron temperature and original density respectively. In such cases, the ion energy spectra extends to infinity, exponentially decaying towards the high energetic end. An isotropic hydrodynamic expansion is seen for such cases [5, 6]. If the electron energies are very high and the laser completely strips the target core of its electrons, then the abundance of positive charges inside the core leads to a violent expansion due to the Coulombic repulsion. The maximum energies of the ions of density n_i, charge Ze attained from the Coulomb explosion of

the target of radius R_t is [7]

$$\varepsilon_C = \frac{4\pi}{3} Z^2 e^2 n_i R_t^2 \tag{4.1}$$

The proton energy distribution $\frac{dN_p}{d\varepsilon} \propto \sqrt{\varepsilon}$ where N_p and ε are the proton number and energy respectively. The proton spectra cuts off at the maximum value of energy ε_C.

In cases where the electron temperature is high enough to break through the restoring charge-separation field of the ions, but not so high to get completely ripped off from the plasma core, neither of the above two expansion regime can define the particle dynamics. In this intermediate regime, the electrons are partially ejected from the core and thus two distinct population of electrons coexist in such cases of ambipolar expansion. A cloud of stripped electrons lead the expansion mechanism and a population of bounded electrons move with the ambient plasma expansion [8]. The ion spectra in such cases features a cutoff energy. In the steep target plasma case the bounded electrons shield the effect of the coulomb repulsion of the core ions and so the maximum value of the ion energies is less compared to a Coulomb exploded case.

The plasma expansion due to the presence of a laser field can be defined by two characteristic scale-lengths: the target plasma radius (R_t) and the hot electron Debye length, $\lambda_{Dh}(t) = \sqrt{\frac{T_h}{4\pi n_e e^2}}$. The solution for the expansion of the protons exists when the ratio of the two scale-lengths, $\Lambda = \frac{R_t}{\lambda_{Dh}}$ is invariant in time [9]. The maximum energy of the protons ε_{max} in a spherical geometry is thus given by [10]

$$\varepsilon_{max} = 2T_h W\left(\frac{\Lambda^2}{2}\right) \tag{4.2}$$

Here, $W(x)$ is the inverse of the Lambert W function, defined as $x(W) = We^W$. The solution asymptotically arrives at the condition for Coulomb explosion case as $R_t \ll \lambda_{Dh}$ with $W(x) \approx x$. On the other hand, the ambipolar expansion state is achieved when $R_t \gg \lambda_{Dh}$ which gives $W(x) \approx$

$ln\left(\frac{x}{lnx}\right)$. The proton distribution function can be expressed as,

$$\frac{dN_p}{d\varepsilon} \propto \sqrt{\frac{\varepsilon}{2T_h}}\left[\frac{1}{\Lambda^2} + exp\left(-\frac{\varepsilon}{2T_h}\right)\right] \tag{4.3}$$

It has been found that both for the low-temperature quasi-neutral expansion and the high-temperature Coulomb explosion scenarios the expansion is isotropic. This effect limits the applicability of the energetic ions attained from such effects. However, for the ambipolar expansion cases, the spherical symmetry of the expansion is broken and it occurs preferentially along the laser propagation direction [11]. However, all these studies were performed using a uniform density plasma target. In this chapter, we used a non-uniform density plasma having gradients inside it to study the expansion mechanisms involved after getting irradiated with a laser-pulse with focus on the generation of energetic ions.

4.2 Simulation parameters

In this work a pulsed femtosecond-long circularly polarized laser is interacted with a spherical hydrogen plasma target having diameter $5\mu m$. The simulations are performed using the 3D PIC code Picpsi-3D [12]. The target sphere is placed at the centre of a simulation box of sides $20\mu m$, so that the sphere centre coincides with the simulation box coordinates $(10, 10, 10)$ in microns. The simulations are carried out with fixed spatial resolutions of 50 nm and absorbing boundary conditions were applied for all six walls for both the fields and particles. Each cell contains 3 macroparticles each for electrons and protons and the temporal resolution is $0.2\omega_p^{-1}$. The laser used has a wavelength of $1\mu m$, so that the critical density is $n_c \simeq 1.112 \times 10^{21} cm^{-3}$. The laser intensity profile is Gaussian in both the transverse directions (X and Y) as well as the longitudinal direction (Z), with the spatial full-width at half maxima (FWHM) being $10\mu m$ and the temporal FWHM being $33fs$. The peak laser intensity is fixed at $3.1 \times 10^{20} Wcm^{-2}$ and correspondingly the normalized vector potential, $a_0 = \frac{eE_0}{\sqrt{2}m_e\omega c} = 15$. Here, E_0 is the peak laser

field amplitude. The plasma is initially considered cold with a Gaussian density variation along the radial direction with a peak density n_{peak} at the centre. Such a density profile could be manipulated by pre-exploding a cryogenic solid hydrogen sphere ($n \approx 6 \times 10^{22} cm^{-3}$) with a laser pulse of lower intensity/ pre-pulse. The density equation is,

$$n(r) = n_{peak} exp\left[-\frac{1}{2}\left(\frac{r}{b}\right)^2\right] \tag{4.4}$$

where r is the distance from the centre of the sphere and $b \approx 0.425\times$ FWHM.

4.3 Results and discussions

To study the expansion profile of the plasma target after the interaction with the laser pulse, its density is kept effectively transparent to the peak intensity of the pulse. Thus, we considered the target with central peak density $n_{peak} \sim \gamma n_c$. By using a target having $n_{peak} = 12 n_c$ and laser parameter, $a_0 = 15$, the critical density layer is $\gamma n_c \simeq 10.65 n_c$. Thus, all but a small volume at the centre of the sphere is relativistically transparent for the laser. As a result, initially, the laser pulse transfers a part of its momentum to the protons located at the core of the target. The high density core experiences a slight push ahead of the centre along the laser axis. From Fig 4.1(a), the proton peak can be seen getting shifted from its initial position at the $10\mu m$ mark of laser propagation direction Z. At a later stage [Fig 4.1(b)], the target expansion plays the dominant role in the proton dynamics and we obtain an exploded target.

It is to be noted that a sharp proton wall is formed at the rear end of the expanded target in Fig. 4.1(b) which gives an element of anisotropicity in the expansion mechanism. Moreover, the high number of electrons present inside the target as seen in Fig 4.2(b) (red line) indicates that the underlying source of expansion in this case is not Coulomb explosion. Quantitatively, the condition for Coulomb explosion is reached when

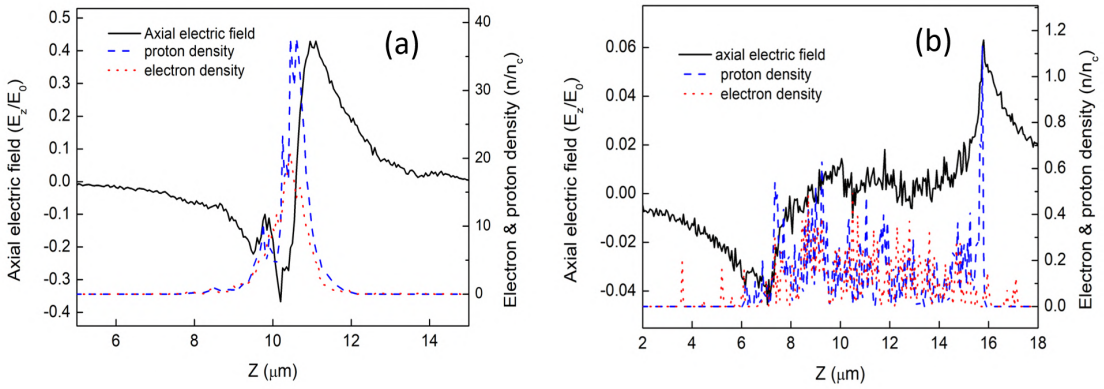

Figure 4.1: The longitudinal electric field (E_z) (black-solid line), proton density (n_p) (blue-dashed line) and the electron density (n_e) (red-dotted line) along the central Z-axis for the plasma target with diameter $5\mu m$, central peak density $n_{peak} = 12n_c$ and the laser parameter $a_0 = 15$ at two different times: (a) 215 fs and (b) 276.3 fs.

$a_0 > \frac{4\pi}{\sqrt{3}}\sqrt{\frac{n_e}{n_c}}\frac{r_T}{\lambda}$ [13]. In our case, Coulomb explosion in the high density core can occur only with laser pulses with $a_0 > 62.9$, which is more than four-times higher than the value considered in our study. Along with it, the fact that the protons remain in close proximity with the electrons as seen in Fig 4.1(b) may suggest ambipolar expansion to have occurred inside the target.

In the present case with target density $12n_c$ i.e. $1.34 \times 10^{21} cm^{-3}$, the Fig. 4.2 indicates that the temperature of the electrons $T_h \approx 7.1 MeV$. Since the target has a radius $R_t = 2.5\mu m = 2.5 \times 10^{-4} cm$, the value of the ratio Λ gives 14.6. Thus, the function $W\left(\frac{\Lambda^2}{2}\right)$ yields 3.123. Therefore, from Eq. 4.2, the maximum proton energy $\varepsilon_{max} \approx 44.3 MeV$. This value is less than the simulated value of maximum energy of the protons. This discrepancy may arise due to the inhomogeneous distribution of density inside the target, which modifies the local debye lengths depending on the target concentration. The proton density snapshot at the central axial plane is shown in Fig. 4.3(a) which shows protons attaining momenta favourably in the laser direction.

The proton energy spectra [Fig 4.3(b)] shows two separate proton population. The first is driven by the expansion of the background protons which is seen from the near-exponential decay in the proton number.

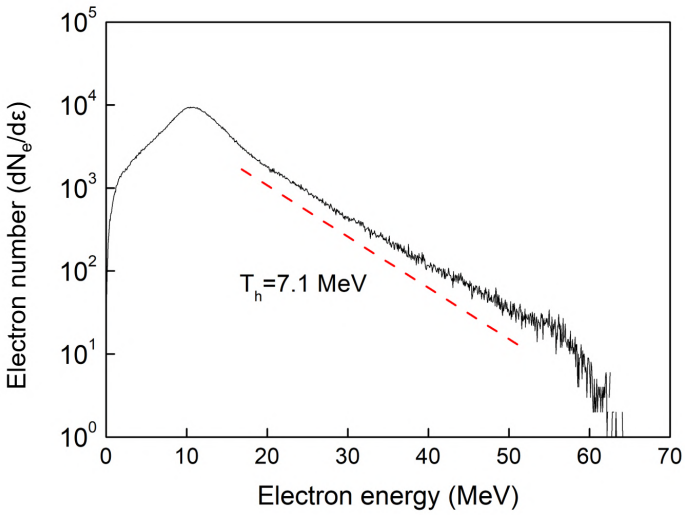

Figure 4.2: The electron energy spectra at 199.5 fs for the case in Fig. 4.1. The dotted line gives the linear fitting for the calculation of electron temperature.

The second population comprises the protons from the high density region that are formed initially near the target centre and that travels forward forming the density spikes as it flows in the ambient plasma having decreasing density gradient. These protons can be seen forming the mono-energetic peaks in the proton spectra at lower energies. The shape of the energy spectra resembles those of the ambipolar expansion.

For comparison, the target diameter is reduced for this case from $5\mu m$

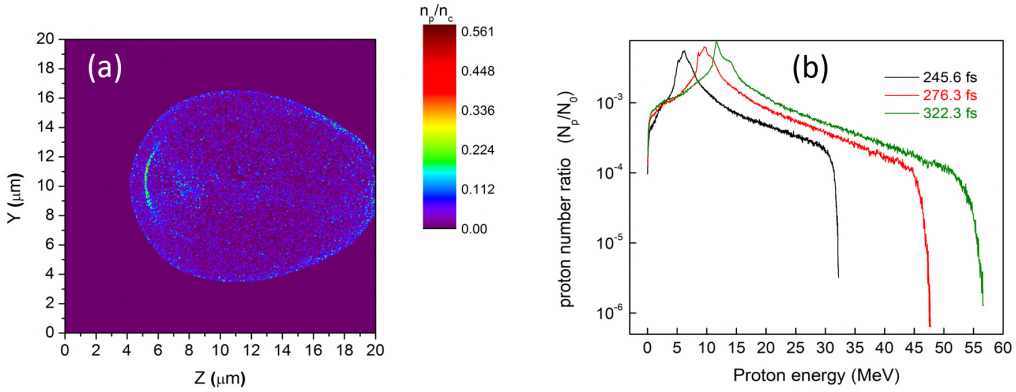

Figure 4.3: (a) The proton density in the central YZ plane at time 322.3 fs and (b) the proton energy spectra at different times denoted by colours for the case with diameter $5\mu m$, $n_{peak} = 12n_c$ and $a_0 = 15$.

to $2\mu m$ and then to $0.5\mu m$, keeping all the other parameters fixed. The

electron density in the central YZ plane are shown in Fig. 4.4(a-c) for the three different target diameters just after the laser peak hits the target. It is seen that for the $5\mu m$ case, almost all the electrons remain cold and are confined to the bulk region. However as the diameter is reduced, the transition from ambipolar to Coulomb explosion regime is distinctly visible. This is consistent to the well established knowledge that Coulomb explosion could be achieved using relatively low intensity laser pulses by decreasing the target diameter. The value of threshold a_0 for Coulomb explosion for the $2\mu m$ diameter case is about 25 which is higher than the present value of a_0 used in this case. However, for the $0.5\mu m$ diameter case, the threshold value for Coulomb explosion is $a_0 \approx 6.3$, and therefore, the Coulomb explosion is attained in the case of the smallest target. The corresponding proton density at later times are shown for the three cases in Fig 4.4(d-f). In the two smaller targets, the protons are expanded in a symmetric manner. The bigger target (diameter $5\mu m$) has a favourable asymmetry along the forward laser direction.

The final energy of the protons at saturation time are shown in Fig. 4.5(a-b) for the three cases. The maximum energy decreases as the diameter of the target is decreased and the shape of the spectra shifts from a nearly ambipolar expansion type (for the first two cases) to a typical explosion case for the smallest target. The asymmetry in the proton direction and distribution as well as the higher maximum energy favours a bigger target which supports the ambipolar expansion as the primary mechanism of proton motion.

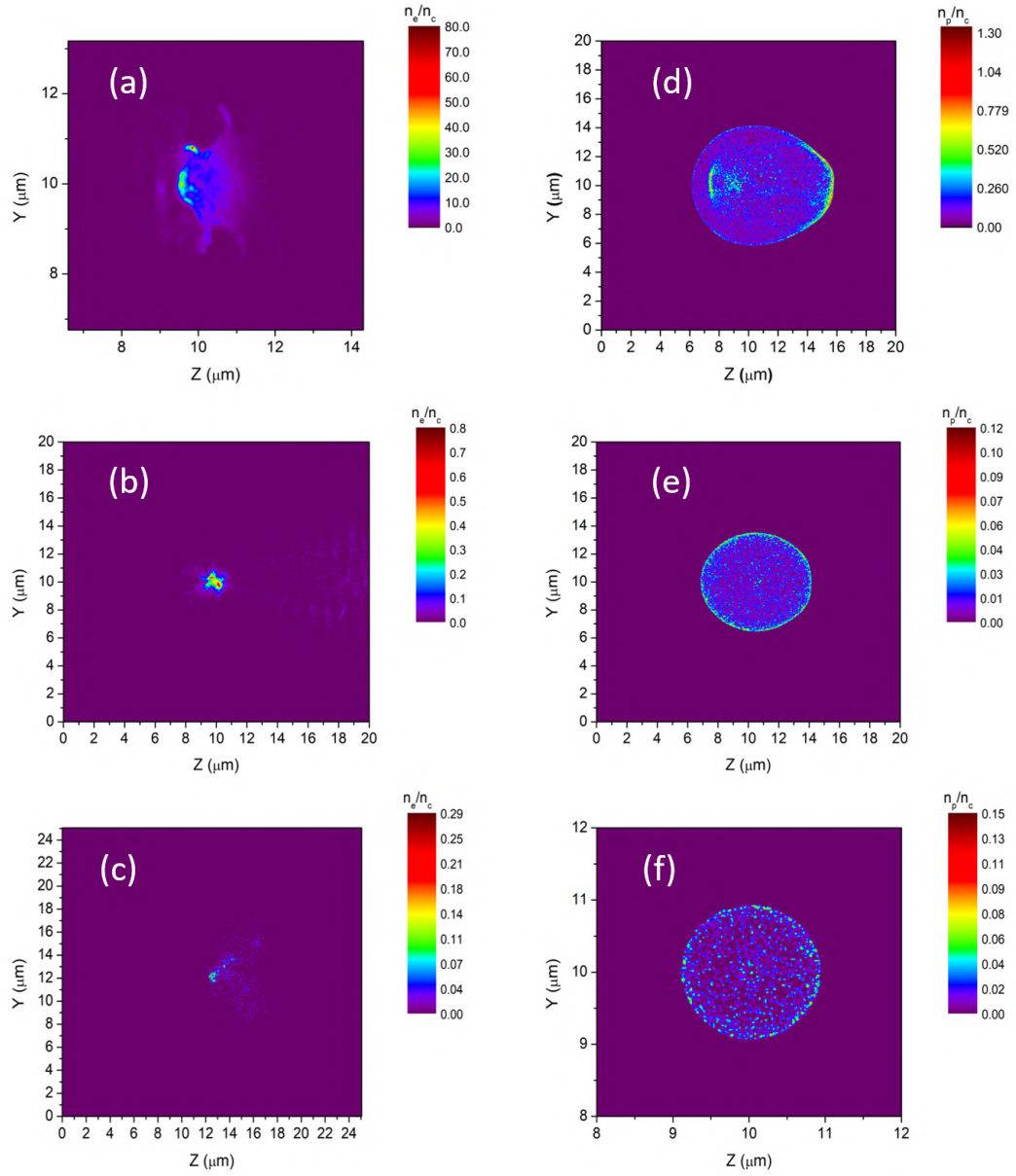

Figure 4.4: The electron density (a-c) and the proton density (d-f) in the central YZ plane. Top row [(a) and (d)]: corresponding figures for the case with diameter $5\mu m$, Middle row [(b) and (e)]: corresponding figures for the case with diameter $2\mu m$. Bottom row [(c) and (f)]: corresponding figures for the case with diameter $0.5\mu m$. In all the three cases, $n_{peak} = 12n_c$ and $a_0 = 15$.

4.4 Conclusion

In this chapter, a Gaussian-type density inhomogeneity is incorporated in the spherical plasma target in the radial direction with the density peaked at the target centre. Using such density modified targets, the tar-

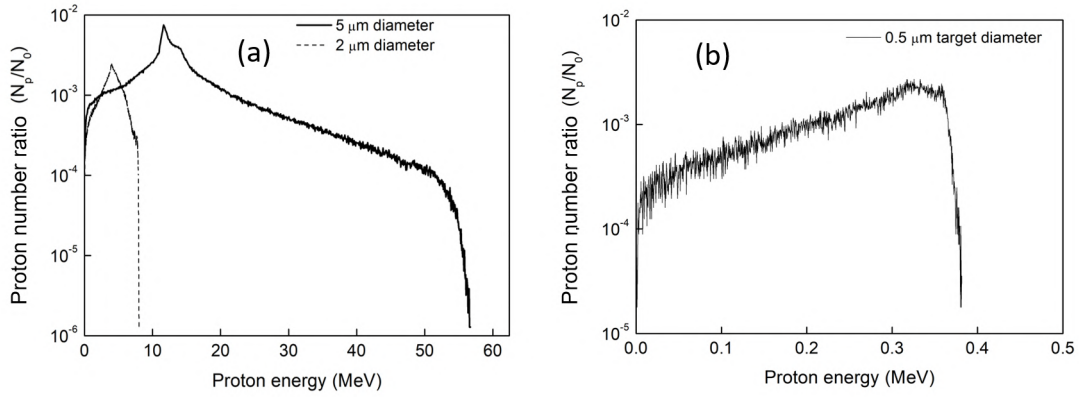

Figure 4.5: The proton energy spectra at the saturation times for the cases with (a) diameter $5\mu m$ (solid line) and diameter $2\mu m$ (dashed line), and (b) diameter $0.5\mu m$.

get expansion due to an intense laser irradiation is studied. The plasma density is kept in the relativistically critical regime to the incoming laser peak intensity so that most of the laser energy is absorbed by the electrons. These electrons acquiring momenta from the laser lead the plasma expansion which in turn drives the ions to high energies. In this chapter we analyse the mechanism of the expansion and identify the target size which may generate an energetic cloud of protons. The results of this chapter may be summarized in the following points:

1. The expansion mechanism of the micron-sized plasma sphere due to the laser action has been identified to be ambipolar expansion. An incomplete removal of the electrons from the core is caused due to the larger size of the plasma.

2. An anisotropicity in the proton expansion is observed in the ambipolar regime. The laser light pressure in the forward direction gives a momentum boost along the direction and causes the asymmetry in the proton cloud. The bigger target favours an asymmetry in the proton direction and distribution as well as a higher maximum energy. The ambipolar expansion acts as the primary mechanism of proton motion.

3. The expansion mechanism shifts from ambipolar to Coulomb explosion when the target size is reduced. Consequently, the asymmetry in the proton dynamics changes to an isotropic expansion of the proton population. Also, it is seen that the maximum energy decreases significantly as the diameter of the target is decreased.

Bibliography

[1] Kluge, T., Enghardt, W., Kraft, S., Schramm, U., Zeil, K., Cowan, T., and Bussmann, M. Enhanced laser ion acceleration from mass-limited foils. *Phys. Plasmas*, 17(12):123103, 2010.

[2] Andreev, A., Okada, T., and Toraya, S. Ultra-intense laser pulse absorption and fast particles generation at interaction with inhomogeneous foil target. In *AIP Conf. Proc.*, volume 634, 303–310. American Institute of Physics, 2002.

[3] Andreev, A., Platonov, K. Y., Okada, T., and Toraya, S. Nonlinear absorption of a short intense laser pulse in a nonuniform plasma. *Phys. Plasmas*, 10(1):220–226, 2003.

[4] Andreev, A., Sonobe, R., Kawata, S., Miyazaki, S., Sakai, K., Miyauchi, K., Kikuchi, T., Platonov, K., and Nemoto, K. Effect of a laser prepulse on fast ion generation in the interaction of ultrashort intense laser pulses with a limited-mass foil target. *Plasma Phys. Control. Fusion*, 48(11):1605, 2006.

[5] Ditmire, T., Donnelly, T., Rubenchik, A., Falcone, R., and Perry, M. Interaction of intense laser pulses with atomic clusters. *Physical Review A*, 53(5):3379, 1996.

[6] Milchberg, H., McNaught, S., and Parra, E. Plasma hydrodynamics of the intense laser-cluster interaction. *Physical Review E*, 64(5):056402, 2001.

[7] Ostermayr, T. *Relativistically Intense Laser–Microplasma Interactions*. Springer, 2019.

[8] Breizman, B. and Arefiev, A. Electron response in laser-irradiated microclusters. *Plasma Physics Reports*, 29(7):593–597, 2003.

[9] Murakami, M. and Basko, M. Self-similar expansion of finite-size non-quasi-neutral plasmas into vacuum: Relation to the problem of ion acceleration. *Physics of plasmas*, 13(1):012105, 2006.

[10] Di Lucchio, L., Andreev, A. A., and Gibbon, P. Ion acceleration by intense, few-cycle laser pulses with nanodroplets. *Phys. Plasmas*, 22(5):053114, 2015.

[11] Symes, D., Hohenberger, M., Henig, A., and Ditmire, T. Anisotropic explosions of hydrogen clusters under intense femtosecond laser irradiation. *Physical review letters*, 98(12):123401, 2007.

[12] Upadhyay, A., Patel, K., Rao, B., Naik, P., and Gupta, P. Three-dimensional simulation of laser–plasma-based electron acceleration. *Pramana*, 78(4):613–623, 2012.

[13] Ostermayr, T. M., Haffa, D., Hilz, P., Pauw, V., Allinger, K., Bamberg, K.-U., Böhl, P., Bömer, C., Bolton, P., Deutschmann, F., et al. Proton acceleration by irradiation of isolated spheres with an intense laser pulse. *Phys. Rev. E*, 94(3):033208, 2016.